

NON-SINGULAR DIRECT FORMULATION OF BOUNDARY INTEGRAL EQUATIONS FOR POTENTIAL FLOWS

W.S. HWANG* AND Y.Y. HUANG

Department of Naval Architecture and Ocean Engineering, National Taiwan University, Taiwan, Province of China

SUMMARY

This paper presents a general direct integral formulation for potential flows. The singularities of Green's functions are desingularized theoretically, using a subtracting and adding back technique, so that Gaussian quadrature or any other numerical integration methods can be applied directly to evaluate all the integrals without any difficulty. When high-order quadrature formulas are applied globally, the number of unknowns can be reduced. Interpolation functions are not necessary for unknown variables in the present paper. Therefore, the present method is much simpler and more efficient than the conventional one. Several numerical examples are calculated and compared satisfactorily with analytical solutions or published results. © 1998 John Wiley & Sons, Ltd.

KEY WORDS: arbitrary-order boundary element method; non-singular formulation; potential problems

1. INTRODUCTION

Since Hess and Smith [1] presented their famous panel methods to solve three-dimensional potential flow problems, numerous schemes have been developed to improve their original work. Meanwhile, another very power numerical method, the finite element method (FEM), was also developed for computational problems in engineering and science. It turns out that many fundamental ideals in FEMs and panel methods are very similar, especially in interpolation techniques. Therefore, panel methods are also called boundary element methods (BEMs) since their panels or elements are distributed on the boundary only, while FEMs have their subdivisions in a whole domain.

In the original panel method, a constant density of source is distributed on each panel, which is called a low-order panel or a constant element. Linear and quadratic functions are then successively developed as interpolation functions in BEMs to promote the accuracy of approximations. Until more recently, cubic splines, B-splines, and cubic B-splines have also been utilized as interpolating functions because they are commonly used for the design of body shapes in industry. Not only source but also vortex and doublet functions are taken as singularity functions and distributed on local boundary elements. All of the mentioned approaches, which determine the strength of singularities at nodal points on the boundary, are

* Correspondence to: Department of Naval Architecture and Ocean Engineering, National Taiwan University, 73 Chow-Shan Road, Taipei, Taiwan 106, Province of China.

called indirect methods. A slightly different formulation, introduced by Morino [2] to solve the velocity potential directly from Green's identity, is called the direct method.

In both formulations of direct and indirect methods, the existence of singularities and dense matrices always greatly increases the computational load when algebraic equations are formed or solved. In order to break up dense matrices, a multi-subdomain scheme is developed to produce an overall system matrix with a sparse blocked character. A sparse matrix saves computer memory and computing time for equation solvers, but it also creates some additional interior boundaries and generates more elements, which can increase the computer effort. However, those interior elements can be eliminated by static condensation in the final form. In general, the multi-subdomain approach is efficient for non-linear or slender computational domain problems [3,4].

When numerical integration is carried out with Gaussian quadrature or any other numerical methods in local elements for BEMs, good accuracy can be achieved with a few integration points if the singular point is not located on the element. However, when the singular point is on the element, the accuracy of numerical quadrature is greatly reduced. Even an increase in the number of Gaussian quadrature points is still of no help when the behavior of integrand is close to the singular point. To solve this difficulty in the numerical integration of singularities, mapping methods were developed by many researchers [5–7]. Usually, different kinds of interpolation functions [7,8] have different analytical forms to be expressed for those singular elements, and such desingularity procedures are complex and lengthy, even for quadratic interpolating polynomials. For higher-order interpolation functions, even analytical expressions are difficult to derive. Only adaptive integration or special numerical quadrature for singular integrals is available. For the overall computational efficiency, these methods may not be completely satisfied.

Besides mapping techniques, other types of non-singular formulations were proposed by researchers [9–14]. In these studies, singular points are moved away from the boundary and outside the computational domain. Such regularization, which results in a Fredholm integral equation of the first kind, may lead to uniqueness and ill-conditional problems of the resulting algebraic equations. In the present study, the definition of the non-singular formulation is different to the previous one. In our formulation, singular points are still on the body surface, but the singular behavior is removed by a subtracting and adding back technique from the Gauss flux theorem. This technique was originally developed by Landweber and Macagno [15] to regularize three-dimensional singularities. The resultant integral equation is a Fredholm integral equation of the second kind, where, in general, no ill-conditional problems occur when the discretized algebraic equations are solved. The difference between the conventional BEM and Landweber's approach is not only in the treatment of singular kernels of the integral equation but also in the numerical procedure for solving solutions. An iterative procedure defined by recurrence formulas was proposed and it solved problems in their studies [15,16]. As indicated by Noblesse [17], the convergence of such an iterative procedure is very fast in the case of longitudinal translation of a slender ellipsoid, but becomes slower when the ellipsoid becomes oblate. Until the limiting case occurs, where an elliptical disk translates in the direction normal to its plane, such an iteration fails to converge.

If the non-singular formulation is utilized for BEMs, no special consideration is necessary for the computation of singular integrals, and the convergence problem due to the iteration procedure in Landweber's approach can also be avoided. When the accuracy is considered, the main errors of BEMs come from interpolation and integration. Since arbitrary functions can be utilized for the shape of bodies in the present approach, the exact body geometry should be used if possible. For the same accuracy of numerical integration, either small elements with

low-order quadrature formula or large elements with high-order quadrature formula can be used. In general, when a high precision integration rule is applied, the required number of total nodes can be less, and in practice, a few large elements are preferred for grid generation. Therefore, larger elements are strongly recommended from both viewpoints of grid generation and numerical integration. In addition, if the points of collocation chosen are exactly the same as those of integration, interpolation functions for unknown variables are not necessary, and it saves computing effort in forming algebraic equations. In the present paper, the shapes of bodies are exact and the whole body is treated as one element for simplicity, although in general, this may not be necessary.

2. THEORY AND FORMULATION

The basic potential flow problem in an unbounded domain is briefly formulated. The fluid is assumed to be inviscid and incompressible, while the flow is assumed to be irrotational. The flow field is described by a velocity potential Φ , which satisfies the Laplace equation within the domain,

$$\nabla^2\Phi = 0, \quad (1)$$

and is subject to the impermeable boundary condition on a body surface,

$$\frac{\partial\Phi}{\partial n} = 0, \quad (2)$$

where n denotes the outward unit normal on a body surface. A boundary integral method involving Green's function may be used to solve the boundary value problem. Before the boundary integral equation is formulated, Green's identity is introduced. Green's identity can be applied over a closed region, relating values of Φ and its normal derivative $\partial\Phi/\partial n$, if Φ is a harmonic function. The potential $\Phi(P)$ at the field point $P(x, y, z)$ can be expressed as

$$\varepsilon\Phi(P) = \int_S \left\{ \Phi(Q) \frac{\partial}{\partial n_Q} [G(P, Q)] - G(P, Q) \frac{\partial\Phi(Q)}{\partial n_Q} \right\} dS_Q, \quad (3)$$

where ε equals 1 when P is inside the domain, $1/2$ when P is on a smooth part of the boundary surface, and zero when P is outside the domain. Q represents the source point (ξ, η, ζ) on the surface S over which the integration is performed, and G is the free space Green's function for Laplace equation.

$$G(P, Q) = \begin{cases} \ln r/2\pi & \text{in two dimensions,} \\ -1/4\pi r & \text{in three dimensions,} \end{cases} \quad (4)$$

where r is the distance between P and Q . By analytical continuation, the exterior incident flow potential Φ_I can be extended into the interior region, so that the interior region is the domain. Then Green's formulation for Φ_I can be expressed as

$$\varepsilon\Phi_I(P) = \int_S \left\{ \Phi_I(Q) \frac{\partial}{\partial n_Q} [G(P, Q)] - G(P, Q) \frac{\partial\Phi_I(Q)}{\partial n_Q} \right\} dS_Q. \quad (5)$$

When the scattering velocity potential, Φ_s , is considered, the domain is in the exterior instead of the interior. Therefore, the coefficient ε in Green's formula should be exchanged, and the scattering velocity potential Φ_s can be expressed in a slightly modified form.

$$(\varepsilon - 1)\Phi_s(P) = \int_S \left\{ \Phi_s(Q) \frac{\partial}{\partial n_Q} [G(P, Q)] - G(P, Q) \frac{\partial \Phi_s(Q)}{\partial n_Q} \right\} dS_Q. \quad (6)$$

The total velocity potential Φ in the exterior region is the summation of the incident potential and the scattering potential,

$$\Phi = \Phi_I + \Phi_s. \quad (7)$$

Adding Equations (5) and (6) and rearranging the result produces the following:

$$(1 - \varepsilon)\Phi(P) = - \int_S \left\{ \Phi(Q) \frac{\partial}{\partial n_Q} [G(P, Q)] - G(P, Q) \frac{\partial \Phi(Q)}{\partial n_Q} \right\} dS_Q + \Phi_I(P). \quad (8)$$

Applying the impermeable boundary condition (2) to Equation (8), when P is on the body surface, gives

$$(\varepsilon - 1)\Phi(P) + \int_S \left\{ \Phi(Q) \frac{\partial G(P, Q)}{\partial n_Q} \right\} dS_Q = \Phi_I(P). \quad (9)$$

Gauss's flux theorem is derived from Equation (3) by setting the velocity potential on S to be constant, then the normal derivative of velocity potential vanishes in the interior region, and we have

$$\int_S \frac{\partial G(P, Q)}{\partial n_Q} dS_Q = \varepsilon. \quad (10)$$

By multiplying Equation (10) with a constant value $\Phi(P)$, then adding Equation (9), we obtain

$$\Phi(P) + \int_S \left\{ [\Phi(Q) - \Phi(P)] \frac{\partial G(P, Q)}{\partial n_Q} \right\} dS_Q = \Phi_I(P). \quad (11)$$

The above equation is used to solve the velocity potential $\Phi(P)$ on S . If the velocity potential is continuous in two-dimensional problems, or if the first derivative of velocity potential along the smooth surface is continuous in three-dimensional problems, the integrand at the left hand side of Equation (11) can be treated as zero when the field point $P(x, y, z)$ approaches the source point $\Phi(\xi, \eta, \zeta)$. Using this modified formulation, those singularities no longer exist in the integral equation and any specially numerical treatments for singularities are no longer needed.

In Equation (2), a stationary boundary condition is assumed in the present paper for simplicity. If a non-stationary boundary condition occurs, a similar procedure to remove the second singular kernel in Equation (8) is also available in Landweber and Macagno [15] by using the theorem of electrostatic capacitance.

3. NUMERICAL PROCEDURE AND RESULTS

In the numerical approach, efficiency is of the most important considerations. A method with less computing points and higher accuracy is preferred. In a one-dimensional integral, Gaussian quadrature is usually a good choice. In a surface integral, minimal-point integration rules or product Gaussian rules are frequently used on each element for BEMs. However, there has been no general formula, until now, for minimal-point integration rules to obtain locations and weighting factors of integration points for an arbitrary precision [18]. Therefore, product Gaussian rules are more convenient if an arbitrarily high-order precision is needed when numerical integration is carried out on a large element.

In Equation (11), the numerical difficulty from singularities has been completely removed, and its integrand can be computed straightforwardly if the geometric data of the surface are known. The information needed for the surface integral is the normal vector and the first fundamental form of surface integral at nodal points. Usually, the body surface is either exactly known or described by approximate functions such as quadratic polynomials, splines, rational polynomials, or any other parametric forms. In traditional BEMs, the same interpolation function is used for both the shape of bodies and unknown variables for every element. In the present paper, those approximate functions are not assumed for unknown variables in the numerical integration.

In our formulation, the locations of collocation points in elements are exactly the same as those for numerical integration nodes. The integral in Equation (11) is discretized into a finite sum at every integration point by the numerical procedure, and the system of algebraic equations is expressed as

$$\sum_{j=1}^N (A_{ij}\Phi_j) = \Phi_{I_i}, \quad (12)$$

where A_{ij} are influence coefficients corresponding to Equation (11), N is the total number of collocation points on all elements, Φ_j is the velocity potential at the j th node, and Φ_{I_i} the incident velocity potential at the i th node. A_{ij} are thereby given by

$$A_{ij} = \begin{cases} -(\vec{r}_{ij} \cdot \vec{n}_j) r_{ij}^{-(1+\alpha)} \omega_j / 2\alpha\pi & j \neq i \\ 1 + \sum_{k=1, k \neq i}^N (\vec{r}_{ik} \cdot \vec{n}_k) r_{ik}^{-(1+\alpha)} \omega_k / 2\alpha\pi & j = i \end{cases} \quad (13)$$

where \vec{r}_{ij} is the vector from the j th node to the i th node, r_{ij} is the distance between the i th and the j th nodes, ω_j is the weighting factor at the j th point from quadrature formulas for surface integral and $\alpha = 1$ in two dimensions, and 2 in three dimensions. The most important feature in Equation (13) is the calculation of A_{ij} , which corresponds to the calculation of singular points in traditional BEMs. Usually, the behavior near singularities needs a special mapping or complex calculation in traditional BEMs. For different interpolation functions, different analytical functions are derived to evaluate the integration of singularities. These complicate expressions frequently take pages in length, and are tedious for programming and computation. In Equation (13), A_{ij} is computed only once for every nodal point when $i \neq j$. A_{ii} needs no additional effort except the summation, because all the terms in the summation are already calculated after A_{ij} , $i \neq j$, are computed. Therefore, it is much more convenient than traditional BEMs for the computation of singular integrals. Furthermore, in traditional BEMs, total influence coefficients must be summed up from all the adjacent elements common to the desired node. In the present method, only the distance between the nodes is computed, and no other interpolation functions need to be evaluated. Therefore, the efficiency of overall computation is improved.

Among the following examples, all the collocation nodes are located at one element only. Although such a distribution may not be the most efficient one, it is the simplest and the accuracy is sufficient for demonstration. The first example in our illustration is for the scattering problem of a uniform flow past an elliptic cylinder, centered at origin, with the major and minor semiaxes, $a = 4$ and $b = 1$, respectively. For a uniform flow of magnitude U along the major axis, a positive x axis, the velocity potential on the ellipse surface can be expressed as

Table I. The values of velocity potential at given nodal points of an ellipse ($a:b = 4:1$)

x/a	Calculated	Analytical
1.00000	1.24994	1.25000
0.92388	1.15480	1.15485
0.70711	0.88384	0.88388
0.38268	0.47833	0.47835
0.00000	0.00000	0.00000
-0.38268	-0.47833	-0.47835
-0.70711	-0.88384	-0.88388
-0.92388	-1.15480	-1.15485
-1.00000	-1.24994	-1.25000

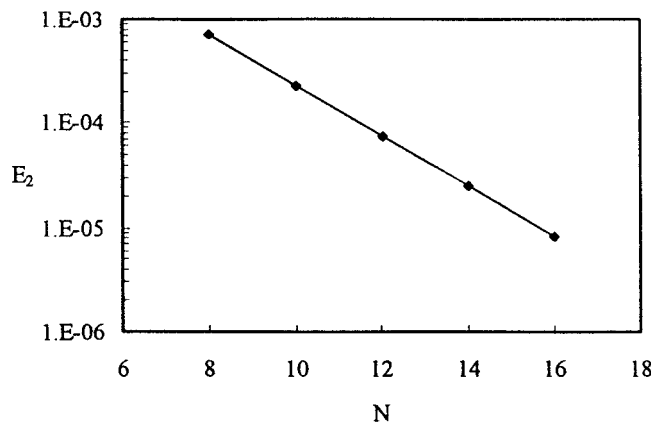
$$\Phi(x, y) = U(a + b)x. \quad (14)$$

In the numerical calculation, 16 nodes are uniformly distributed on the ellipse surface along the polar angle ($0 \leq \theta < 2\pi$), and the trapezoidal rule is selected for integration. Since the flow is symmetrical about x -axis, only the result on the upper ellipse is listed in Table I.

In comparison with the results of Shultz and Hong [13], the root mean square errors (E_2) of 128 computed points for the same ellipse are $-\log_{10}E_2 = 2.94, 2.90$ and 4.12 for weak, strong, and over-determined systems, respectively. In this study, $-\log_{10}E_2 = 5.08$ with 16 computed nodes as shown in Figure 1. In fact, if the body surface is smooth, the kernel of Equation (11) for two-dimensional problems is continuous along the boundary. When the even spacing trapezoidal rule is applied for such integrals, the error of numerical integration decays exponentially in theory. Therefore, for the same accuracy, the required computed nodes in our formulation can be much less.

The second example in our illustration is for the scattering problem of a two-dimensional flow along the major axis of an ogive in which its surface is not smooth. The definition of the ogives is given in equation (15) [17]

$$\begin{aligned} |x| &= (1 - t^2)/(1 + t^2 + 2t(1 - b^2)/(1 + b^2)), \\ |y| &= 4bt/(1 + b^2)/(1 + t^2 + 2t(1 - b^2)/(1 + b^2)), \end{aligned} \quad (15)$$

Figure 1. Root mean square errors of velocity potentials for an ellipse ($a:b = 4:1$).

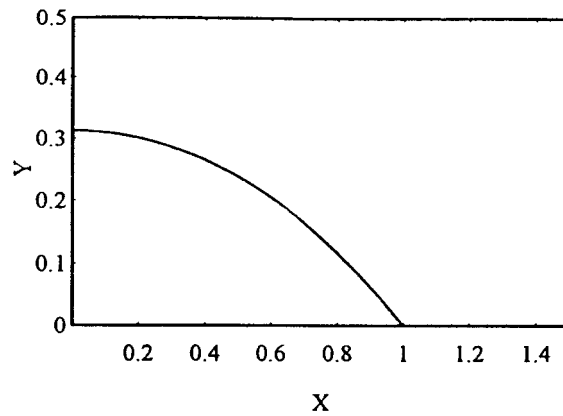


Figure 2. The shape of a quarter ogive with $b = 1/4$.

where b is the thickness ratio ($0 \leq b \leq 1$), and $t = [\tan(\lambda/2)]^\delta$ with $\delta = 2[1 - (2/\pi) \tan^{-1} b]$ and the parameter λ varies between 0 and $\pi/2$. Ogives are symmetric about both x and y axes, so 1/4 of the ogive with $b = 0.25$ is plotted in Figure 2. The total potential on the surface of an ogive is given by Equation (16) [17]

$$\phi = \frac{x}{|x|} \cos \lambda \left/ \left(1 - \frac{2}{\pi} \tan^{-1} b \right) \right. \tag{16}$$

Because of the symmetry, computed nodes are distributed on the first quadrant only. Because the ogive is not smooth at the ends, the normal vectors of both ends do not exist. Therefore, Gaussian quadrature formulas without end points are selected to evaluate these numerical integrations. The root mean square errors (E_2) between the computed and exact values are shown in Figure 3 for different numbers of nodes. Although the speed of convergence no longer decays exponentially, the high-order algebraic convergence still maintains.

Other examples are for the scattering problems of a uniform flow past a sphere and an ellipsoid, respectively. Because of symmetry about the $x-z$ and $x-y$ planes, only 1/4 of the surface is calculated. In the third example, the sphere of radius a is calculated with 8×4

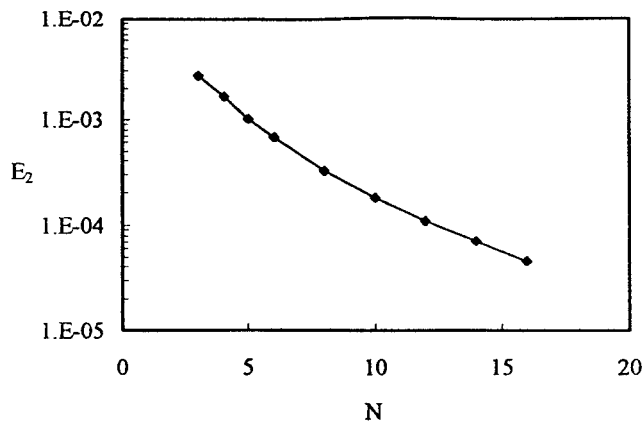


Figure 3. Root mean square errors of velocity potentials for the ogive with $b = 1/4$.

Table II. The values of velocity potential at given nodal points of a sphere

x/a	Calculated	Analytical
0.93057	1.39463	1.39585
0.66999	1.00462	1.00499
0.33001	0.49566	0.49501
0.06943	0.10527	0.10415
-0.06943	-0.10527	-0.10415
-0.33001	-0.49566	-0.49501
-0.66999	-1.00462	-1.00499
-0.93057	-1.39463	-1.39585

Gaussian points. Both analytic and calculated results of the non-dimensional velocity potential on the sphere surface are listed in Table II. The same problem was solved recently by Zang *et al.* [7], by using 161 nodal points for the quadratic element and 209 nodal points for the linear element on a quadrant of a sphere surface to obtain about the same order of accuracy, the fourth decimal digit, with the same result as in this study. Therefore, comparing results with quadratic elements in the conventional method for the same accuracy, the number of required nodes on a quadrant of a sphere surface in our case is about 1/10.

The last example is an ellipsoid with three semi-axes, $a = 4$, $b = 1$ and $c = 2$. Gaussian points (16×8) are distributed over 1/4 of the ellipse surface. The analytic solution on the elliptic surface can be found in the hydrodynamic book by Milne-Thompson [19].

$$\Phi(x, y, z) = 1.12657 Ux. \quad (17)$$

The analytical and computational results of the velocity potential on the ellipsoidal surface are compared in Table III, and the accuracy is up to the fourth decimal digit. All these examples confirm the great accuracy of the present method.

Table III. Potential values at given nodal points of an ellipsoid (4:1:2)

x/a	Calculated	Analytical
0.98014	1.1049	1.1042
0.89833	1.0120	1.0120
0.76277	0.8594	0.8593
0.59172	0.6667	0.6666
0.40828	0.4600	0.4600
0.23723	0.2673	0.2673
0.10167	0.1146	0.1145
0.01986	0.0224	0.0224
-0.01986	-0.0224	-0.0224
-0.10167	-0.1146	-0.1145
-0.23723	-0.2673	-0.2673
-0.40828	-0.4600	-0.4600
-0.59172	-0.6667	-0.6666
-0.76277	-0.8594	-0.8593
-0.89833	-1.0121	-1.0120
-0.98014	-1.1049	-1.1042

4. CONCLUSIONS

A non-singular direct formulation of boundary integral equation for potential flows is presented. In two-dimensional flows, if a body is smooth, errors of numerical integration decay exponentially when the trapezoidal rule is applied, and the solution also converges exponentially. If the body is not smooth, then the solution is still of high-order convergence when Gaussian quadrature is applied. In three-dimensional flows, the total number of nodal points for a smooth body can be reduced by one order in the test case when comparing with the conventional method for the same accuracy. Therefore, the boundary element method is much improved in the present formulation. In addition, since no special numerical treatment for singularities, and no interpolation functions for integration is needed, the present method greatly reduces the total computational procedure.

REFERENCES

1. J.L. Hess and A.M. Smith, 'Calculation of nonlifting potential flow about arbitrary three-dimensional smooth bodies', *J. Ship Res.*, **7**, 22–44 (1964).
2. L. Morino and C.C. Kuo, 'Subsonic potential aerodynamics for complex configurations: a general theory', *AIAA J.*, **12**, 191–197 (1974).
3. J.H. Kane, *Boundary Element Analysis*, Prentice Hall, New Jersey, 1994.
4. P. Wang, Y. Yao and M.P. Tulin, 'An efficient numerical tank for non-linear water waves, based on the multi-subdomain approach with BEM', *Int. j. numer. methods fluids*, **20**, 1315–1336 (1995).
5. J.C. Lachat and J.O. Watson, 'Effective numerical treatment of boundary integral equations: a formulation for three-dimensional elasto-statics', *Int. j. numer. methods eng.*, **10**, 991–1005 (1976).
6. F.J. Rizzo and D.J. Shippy, 'An advanced boundary integral equation method for the three-dimensional thermo-elasticity', *Int. j. numer. methods eng.*, **11**, 1753–1768 (1977).
7. Y.L. Zang, Y.M. Cheng and W. Zhang, 'A higher-order boundary element method for three-dimensional potential problems', *Int. j. numer. methods fluids*, **21**, 311–321 (1995).
8. J.N. Newman, 'Distributions of source and normal dipoles over a quadrilateral panel', *J. Eng. Math*, **20**, 113–126 (1986).
9. W.C. Webster, 'The flow about arbitrary three-dimensional smooth bodies', *J. Ship Res.*, **19**, 206–218 (1975).
10. U. Heise, 'Numerical properties of integral equation in which the given boundary values and the solutions are defined on different curves', *Comput. Struct.*, **8**, 199–205 (1978).
11. P.S. Han and M.S. Olson, 'An adaptive boundary element method', *Int. j. numer. methods eng.*, **24**, 1187–1202 (1987).
12. R.L. Johnson and G. Fairweather, 'The method of fundamental solutions for problem in potential flow', *Appl. Math Modeling*, **8**, 265–270 (1984).
13. W.W. Schultz and S.W. Hong, 'Solution of potential problems using an overdetermined complex boundary integral method', *J. Comput. Phys.*, **84**, 414–440 (1989).
14. Y. Cao, W.W. Schultz and R.F. Beck, 'Three-dimensional desingularized boundary integral methods for potential problems', *Int. j. numer. methods fluids*, **12**, 785–803 (1991).
15. L. Landweber and M. Macagno, 'Irrotational flow about ship forms', *IHHR report*, Iowa, No. 123, 1969.
16. S.K. Chow, A.Y. Hou and L. Landweber, 'Hydrodynamic forces and moments acting on a body emerging from an infinite plane', *Phys. Fluids*, **19**, 1439–1449 (1976).
17. F. Noblesse and G. Triantafyllou, 'Explicit approximations for calculating potential flow about a body', *J. Ship Res.*, **27**, 1–12 (1983).
18. P.J. Davis and P. Rabinowitz, *Methods of Numerical Integration*, Academic Press, New York, 1984.
19. L.M. Milne-Thompson, *Theoretical Hydrodynamics*, Macmillan, London, 1960.